Preprint
UCRL-JC-138315

The Potential of Fast Ignition and Related Experiments with a Petawatt Laser Facility

M.H. Key, E.M. Campbell, T.E. Cowan, S.P. Hatchett,
E.A. Henry, J.A. Koch, A.B. Langdon, B.F. Lasinski, A. MacKinnon,
A.A. Offenberger, D.M. Pennington, M.D. Perry, T.J. Phillips,
T.C. Sangster, M.S. Singh, R.A.Snavely, M.A. Stoyer,
M. Tsukamoto, K.B. Wharton, S.C. Wilks

This article was submitted to
1999 Symposium on Cost-Effective Steps to Fusion Power, Washington, D.C., March 25, 2000

April 6, 2000

U.S. Department of Energy
Lawrence Livermore National Laboratory

THE POTENTIAL OF FAST IGNITION AND RELATED EXPERIMENTS WITH A PETAWATT LASER FACILITY

M. H. Key, E. M. Campbell, T. E. Cowan, S. P. Hatchett, E. A. Henry
J. A. Koch, A. B. Langdon, B. F. Lasinski, A MacKinnon
A. A. Offenberger*, D. M. Pennington, M. D. Perry, T. J. Phillips
T. C. Sangster, M S. Singh, R A. Snavely, M. A. Stoyer, M. Tsukamoto**, K B. Wharton, S. C. Wilks.

Lawrence Livermore National Laboratory, P.O. Box 808, L-473
Livermore CA 94550 USA

*Visiting from Department of Electrical Engineering, University of Alberta, Edmonton, Alberta, T6G 2G7, Canada

**Visiting from Joining & Welding Research Institute, Osaka University, Ibaraki, Osaka 567, Japan

ABSTRACT

A model of energy gain induced by fast ignition of thermonuclear burn in compressed deuterium-tritium fuel, is used to show the potential for 300x gain with a driver energy of 1 MJ, if the National Ignition Facility (NIF) were to be adapted for fast ignition.

The physics of fast ignition has been studied using a petawatt laser facility at the Lawrence Livermore National Laboratory. Laser plasma interaction in a preformed plasma on a solid target leads to relativistic self-focusing evidenced by x-ray images. Absorption of the laser radiation transfers energy to an intense source of relativistic electrons. Good conversion efficiency into a wide angular distribution is reported. Heating by the electrons in solid density CD_2 produces 0.5 to 1keV temperature, inferred from the D-D thermo-nuclear neutron yield.

1. INTRODUCTION

The concept of Fast Ignition (FI) [1] is of importance in inertial fusion energy (IFE) research because it offers the possibility of significantly higher gain than can be obtained in indirectly driven [2] or directly driven [3] inertially confined fusion (ICF). Higher gain would allow power generation with lower driver efficiency or lower recirculating power fraction and FI is, therefore, attractive for conceptual laser driven IFE power plants. Figure [1] compares the calculated gain for ICF targets of a

size appropriate to the 1.8 MJ National Ignition Facility (NIF) now being constructed at the Lawrence Livermore National Laboratory. The NIF ignition target designs for indirect drive have been developed over decades of research and there is a sound basis for the predicted gain factor of 12 to 20. The research base for direct drive with predicted gains at NIF scale of 20 to 70 is less mature, but is, nevertheless, substantial. The gain of about 300 indicated for FI at NIF scale is based on a simple model discussed here in Section 2. The potential of FI is evident but its feasibility depends on the newer physics of the interaction of intense laser radiation with plasma in the relativistic regime and remains to be proven.

2 FAST IGNITION MODEL AT THE SCALE OF NIF

The essential idea of fast ignition is to pre-compress the fusion fuel by conventional laser driven methods, then to ignite the fuel with a separate short duration high intensity laser pulse. A pre-cursor hole boring pulse creates a channel in the plasma atmosphere enabling the ignitor pulse to penetrate close to the dense fuel. Absorption of the ignitor pulse at the critical density interface generates a beam of relativistic electrons, which transports energy to the dense fuel and heats the ignition spark.

The energy required to be delivered to the ignition spark by the electron beam has been determined from numerical simulations [4] and can be written in the form 80 $(100/\rho)^{1.8}$ kJ where ρ is the fuel density in gcm^{-3}. The same analysis shows the requirements for temperature kT=10keV and density radius product $\rho r = 0.5$ g cm^{-2}. Reducing the density, therefore, proportionally increases both the spark radius and its inertial confinement time, the latter being proportional to the radius. Assuming that the laser focal spot area is proportional to the ignition spark area, the intensity in the focal spot is proportional to ρ. The electrons are required to have an energy deposition range equal to the spark ρr. A limit of about 1 MeV is, therefore, imposed on their energy. The laser intensity x (wavelength)^2 or $I\lambda^2$ determines the ponderomotive potential and thus the closely related energy of the electrons [5]. $I\lambda^2$ is required to be approximately $2.5 \times 10^{19} Wcm^{-2}\mu m^2$.

Figure 1 shows how these constraints can be met at the scale of NIF for a fuel density of $200gcm^{-3}$ with 10% of the NIF beams adapted for chirped pulse amplification (CPA)[6]. Conversion at 60% efficiency to 0.53 μm wavelength is assumed in order to help meet the $I\lambda^2$ constraint, giving a total short pulse energy of 200 kJ. The beams would be focused to a clustered array of 25 μm diameter spots at 20 ps pulse duration for 200 gcm^{-3} density; giving the $I\lambda^2$ value shown in figure 1. It is further assumed that hole boring brings the ignitor beams to within about 100 μm of the dense fuel where there is 30% conversion to electrons. Energy transfer by the electron beam to the ignition spark with self induced magnetic collimation [6] is assumed to be 66% efficient with a two fold increase in electron beam diameter between the optical focal spot and the ignition spark. Compression of the fuel is assumed to be with 8% hydrodynamic efficiency typical of direct drive, and with a ratio α=2 of internal energy to the Fermi degenerate minimum. The gain is computed by specifying the fuel density and varying the fuel mass. Summing the required primary laser energy delivered to ignitor beams and the laser energy needed for fuel compression gives the total laser energy input. The fusion burn output is calculated from the burn efficiency $\rho r/(\rho r+7gcm^{-2})$ and the fuel mass. For example, if 1 MJ of laser energy is used to compress the fuel, the fuel mass is 4.1 mg with a diameter of 340 μm. the ρr is 3.4 gcm^{-2} and the burn efficiency is 0.33. The gain i.e. ratio of burn yield to laser energy is, therefore 330.

It is necessary for obtaining high gain that the total laser driver energy be well above the ignition threshold and this sets a lower limit on the density as illustrated in figure 1 because the threshold energy increases as $\rho^{-1.85}$. The upper density limit arises from $I\lambda^2$ in the focal spots, which increases approximately linearly with density as indicated in figure 1. In this scenario there is an operating window centered at about 200 gcm^{-3}.

The higher gain obtained in fast ignition arises because we assume a high compression efficiency η=8%, characteristic of direct drive, a low adiabat ratio α=2 and a low density

ρ=200 gcm^{-3}, where the energy used to compress the fuel dominates the total input energy and scales as $\eta\alpha\rho^{2/3}$. A low fuel adiabat is easier to achieve in fast ignition because the fuel density and pressure are reduced and there is no need for a central hot spot with its associated sensitivity to hydro-instabilities. Lower value of ρ relative to direct drive is the primary source of the higher gain for FI shown in figure 1.

This simple model has many limitations. The requirement in fast ignition research is to substantiate that the postulated behaviors can be obtained, in particular the efficient transfer of energy from the ignitor laser beam to the ignition spark. It is apparent that if they can be obtained, then fast ignition has a unique capability for high gain of considerable potential importance for IFE.

3. THE PETAWATT LASER at LLNL

One beam line of the 10 beam Nova laser using disc amplifiers of up to 31.5 cm diameter, was adapted for chirped pulse amplification (CPA) [8] to generate up to 0.8 kilojoule in a stretched pulse. Petawatt power was obtained by recompressing the stretched pulse to a minimum duration of less than 500 ps, using a pair of 1 meter diameter reflection gratings. A computer controlled deformable mirror (DM) improved the wavefront as illustrated in figure 2. A typical image without the DM after a 7 hour cooling delay, shows significant thermal distortions. The improved focal spot shown with use of the DM was reproducible for firing intervals as short as 1 1/2 hours. Analysis of the ccd images gave a determination of the spectrum of intensity. Typically, peak intensities reached values up to 3 x10^{20} Wcm^{-2} for f/3 focussing when the laser was operated at a power of 1 PW. 20% of the energy was delivered at intensities above 10^{20} Wcm^{-2}. The fraction of the power contained up to the first minimum around the central focal spot was 30%. The Strehl ratio was 5% and the fwhm of the central focal spot was 2.5 times the diffraction limit.

There was laser energy incident on the target prior to the arrival of the short-pulse, due to amplified spontaneous emission (ASE) and small fractional leakage of the short-pulse through Pockels cell gates in the pulse generator system. ASE began approximately 4 ns prior to the short

pulse at a roughly constant intensity and its energy was typically 3 x10^{-4} of the main pulse energy. A leakage pulse arrived 2 ns before the main pulse and its minimized energy was 10^{-4} of the main pulse.

4. Relativistic channeling

The ASE and leakage pre-pulse created a preformed plasma from solid targets prior to the arrival of the main pulse. Interaction of the main pulse with this plasma particularly by relativistic self-focusing was important in the conversion of laser energy to electron energy. Short-pulse optical interferometry was used to measure the density structure of the pre-pulse induced plasma and these results have been compared with numerical simulations in 2 dimensional cylindrical symmetry using the hydrodynamic code Lasnex [9]. There was good consistency of measured and computed results with the approximately exponentially falling density profile having a scale length of 40 micron.

Evidence of relativistic channel formation [10] is shown in figure 3. The laser was focused at variable distances in front of and behind the surface of a planar Au target at normal incidence at energy of 550 J in 0.5 ps. The irradiated area on the target (assuming the propagation of the laser to be unaffected by the pre-formed plasma) is shown by the superimposed circles. For focusing 300 μm in front of the target, the x-ray pinhole camera image of the front surface of the target (filtered to record x-rays of about 5 keV energy), shows an emission zone, which is approximately 20 μm in diameter and much smaller than the nominal 100 micron diameter irradiated area. The image has structure, suggesting one strong filament and 2 subsidiary filaments. Displacement of the target to the plane of best focus shows an essentially invariant x-ray image. When the laser was focused 200 μm behind the surface, the x-ray image was diffused and of weak intensity extending over more than 300 μm diameter. It had one 10 μm diameter bright spot attributable to a small local region of the undergoing relativistic self-focusing. The yield of photo-neutrons [11] was essentially invariant at 2 to 3 x10^{8} for focusing in front of the target while focusing behind the target surface gave a drop in

yield to 10^7. The neutron data support the scenario suggested by the x-ray images by implying invariant higher intensity for focussing in front of the target attributable to relativistic filaments.

5. CONVERSION EFFICIENCY AND ANGULAR DISTRIBUTION OF THE ELECTRONS

Conversion of up to 30% of the incident laser energy into electrons of mean energy exceeding 600 keV has been inferred from measurements the Kα fluorescence of a buried layer of Mo in Cu targets [12]. These measurements made at peak focused intensity of $2x10^{19}$ Wcm^{-2} in 0.5 ps pulses were obtained with 15 J laser pulses using a smaller scale prototype of the PW beam. Increasing conversion at higher intensities was noted in scaling studies [13].

The total yield of bremsstrahlung x-rays from 1mm thick Au targets at photon energy >0.5 MeV was determined for 1PW laser pulses using an array of 150 filtered thermoluminescent (TLD) detectors covering the forward hemisphere. 11 J of X-rays equivalent to 2.9 % of the laser energy was recorded. This was estimated to correspond to 40 to 50% conversion of laser energy to electrons by using Monte Carlo modeling with the Integrated Tiger Series code (ITS) [14].

X-ray bremsstrahlung from relativistic electrons has a cone angle of $1/\gamma$ where γ is the relativistic factor. Consequently, measurements of the angular distribution of the x-ray emission at photon energies in the MeV region are almost equivalent to direct measurement of the angular distribution of the electron flux in the target. The array of thermo-luminescent (TLD) detectors produced a hemisphere map of x-ray emission with a broad angular range with a full width at half maximum (fwhm) of 180° and a variable direction of the peak

Higher energy x-ray photons interacting with high z target materials induce photo-neutron emission (γ, xn) and nuclear activation through nuclear giant resonances [11,15]. The x=1 process in Au was used to map the angular pattern of higher energy photons of about 15 MeV where the cross section peaks. 31 Au discs covering the forward hemisphere were used as activation detectors. There

was a characteristic 100° fwhm of the angular pattern illustrated in figure 4, but the direction of the peak was random over an 80° range.

6. Mechanisms Influencing the Electron Source

Possible causes for the stochastic directional behavior and the wide beam divergence of the x-ray emission and the electron source include a hosing instability of the relativistic filament at near critical density, which has been seen in particle in cell (PIC) modeling [16] and Weibel instability breaking up the relativistic electron current into multiple off axis filaments which has also been seen in PIC modeling [17]. Refraction and multiple filamentation in the structure of preformed plasma may also contribute.

7. Heating by the Electrons

The wide angle pattern of the electron source is disadvantageous for fast ignition, but may be mitigated by self induced magnetic collimation of the electron beam in solid density matter suggested by recent theoretical work [6,18] and optical probing experiments [20]. Specific calculations [18] for intensity of 2×10^{19} Wcm^{-2} in a 15 μm focal spot show collimated heat flow with temperature reaching 3 keV on axis and 1keV out to a radius of 15 μm penetrating through 0.1mm of solid CD_2. This kind of heat transport is highly desirable for fast ignition. Experiments within buried layers of Al in CH have given interesting indications of heating to about 300eV in a collimated pattern [20].

Evidence of temperature of 500 ev to 1 keV due to heating by relativistic electrons was obtained from observation of thermonuclear D-D reactions in solid CD_2.
Thermonuclear fusion reactions in CD_2 generate neutrons from DD fusion with an energy of 2.45 MeV and an energy spread in keV of $82(kT/1keV)^{1/2}$. Such nearly mono-energetic thermal neutron emission is very different from the photo-neutron emission discussed earlier or neutron generation by accelerated deuterons striking static deuterons [21], or (p, n) process from fast protons striking the target chamber walls, all of which produce neutron energy spectra that are many MeV wide. Figure 5 shows a neutron spectrum recorded by a large aperture neutron scintillator array (Lansa) comprised of

960 photo-multiplier/scintillator detectors located 21.5 m from the target at an angle that is backward at 70^0 from the laser axis. The target had 10 μm CH over 100 μm CD_2 and was irradiated at 5 ps with 180J. The striking feature of the spectrum is a narrow peak at 2.45 MeV superimposed on a broad background. Statistical analysis shows that this peak is at 4 standard deviations relative to the statistical noise in the spectrally broad background signal and can therefore be attributed to thermonuclear reactions. The peak implies emission of 6×10^4 thermo-nuclear neutrons. This experiment was at the statistical limit for detection of the narrow thermal peak in the spectrally broad background of neutrons produced other processes and in multiple shots and it was seen only occasionally. Such random behavior is consistent with the number of thermonuclear neutrons being close to the statistical noise level of the broad spectrum and with a strong (T^5) scaling with temperature. The yield of neutrons suggests heating to a temperature of 0.5 to 1 keV.

CONCLUSIONS

Fast ignition has been shown to have a significant potential advantage of higher gain, which at the NIF relevant level of 1MJ drive reaches 300x. Experiments with the PW laser have shown evidence of relativistic self-focusing with efficient conversion to a rather wide-angle beam of relativistic electrons. Observation of D-D thermonuclear fusion suggests heating of solid CD_2 to temperatures of 500 eV to 1 keV.

*Work performed under the auspices of the U.S. Department of Energy by the Lawrence Livermore National Laboratory under Contract No. W-7405-ENG-48.

[1] M. Tabak, J. Hammer, M.E. Glinsky, W.L. Kruer, S.C. Wilks, J. Woodworth, E.M. Campbell, M.D. Perry, Phys Plasmas, 1, 1626 (1994)
[2] J.D. Lindl, Laser Interaction and Related Plasma Phenomena, AIP Conf. Proc. 318, p. 635 (1993)
[3] S. E. Bodner, D.G. Colombant, J.H. Gardner, R.H. Lehmberg, S.P. Obenschain, L. Phillips, A.J. Schmitt, J.D. Sethian, R. L. McRory, W. Seka, C.P. Verdon, J.P. Knauer, B.B. Afeyan, H.T. Powell, Phys. Plasmas, 5, 1901 (1998)
[4] S. Atzeni Jpn. J. Appl. Phys. 34, 1980 (1995), and S. Atzeni Proc. 2nd Int. Workshop on Fast Ignition Publ. Max Planck Inst. fur Quanten Optik (1997)
[5] S.C. Wilks, Phys. Fluids B52, 603 (1993)

[6] M. D. Perry and G Morou, Science, 264, 917 (1994)
[7] J. R. Davies, A. R. Bell, M. G. Haines, S. Guerin, Phys. Rev. E 56, 7193 (1997)
[8] M. D. Perry et al. Opt. Letts. 24, 160 (1999)
[9] G. B. Zimmermann and W. L. Kruer, Comments on Plasma Phys. and Contr. Fusion 11,51 (1975)
[10] M. Borghesi et al. Phys. Rev. Lett. 78, 879 (1997)
[11] T.W. Phillips, et al. Rev Sci. Instr. 70, 1213 (19999)
[12] K. L. Wharton, S. P. Hatchett, S. C. Wilks, M. H. Key, J. D. Moody, V. Yanovski, A. A. Offenberger, B. A. Hammel, M. D. Perry, C. Joshi. Phys. Rev. Lett. 81, 822 (1998)
[13] M. H. Key et al. Phys. Plasmas. 5, 1996 (1998)
[14] S. P. Hatchett et al. Phys. Plasmas, May (1999) (in press)
[15] T. E. Cowan et al. Phys. Rev. Lett., 84, 903, 2000
[16] B. Lazinski, A.B. Langdon, S.P. Hatchett, M.H. Key, M. Tabak, Phys. Plasmas (to be published)
[17] J.C. Adam et al. Proc. 3rd Int. Workshop on Fast Ignition, Publ. Rutherford Appleton Lab. (1998)
[[18] J. R. Davies, A.R. Bell, M Tatarakis, Phys. Rev. E, 59, 6032 (1999)
[19] L. Gremillet et al., Phys. Rev. Lett. 83, 5015 (1999)
[20] J.A. Koch et al., Lasers and Part. Beams, 16, 225 (1998) and J A Koch et al., Phys. Rev. E. (submitted)
[21 L Disdier, J.P. Garconnet, G. Malka, J.L. Miquel. Phys. Rev. Letts. 82, 1454, (1999)

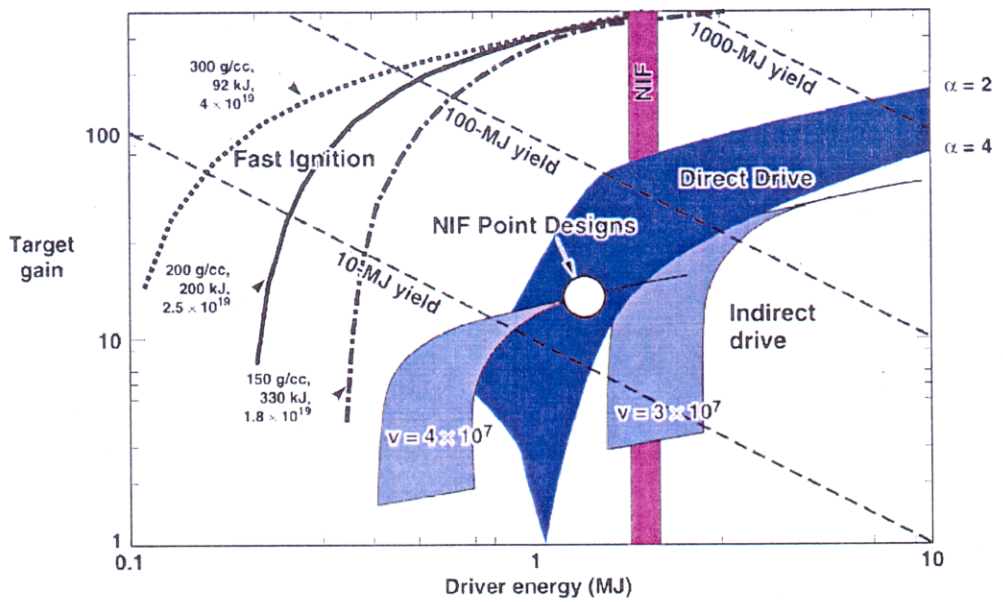

FIG.1. Calculated gain curves for laser driven ICF targets. Fast *ignition plots are labeled with density, ignition spark driver energy and focal spot* $I\lambda^2$.

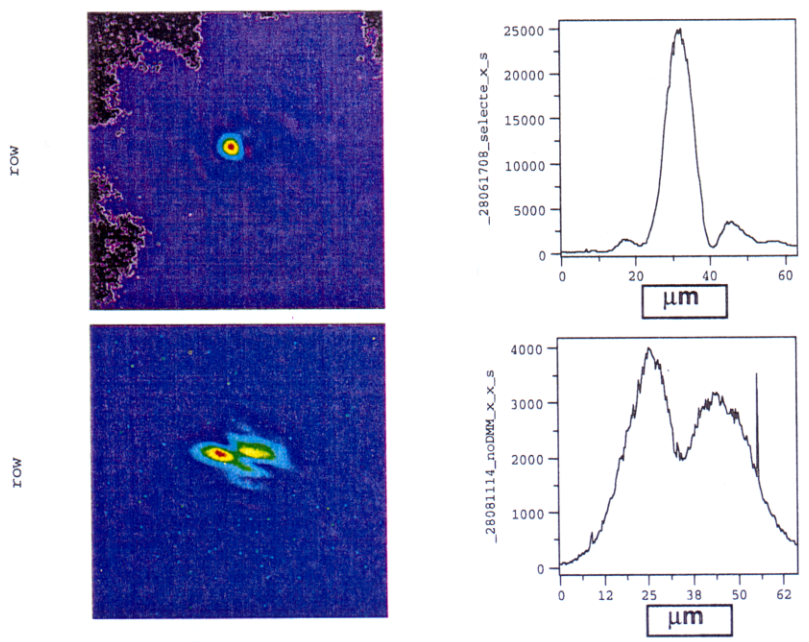

FIG. 2. Equivalent plane focal spot images and horizontal lineouts with (above) and without (below) the deformable mirror (DM). The f.w.h.m. of the focal spot with the DM is 8 µm.

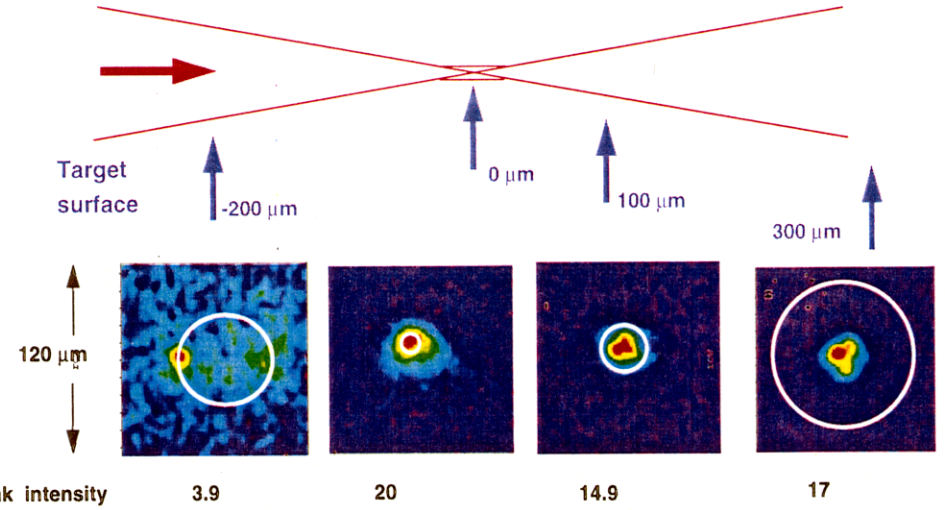

FIG. 3. X-ray pinhole camera images. The location of the target surface relative to the focal plane is indicated in the sketch. White circlse denots the size of the beam at the target surface in the absence of any plasma.

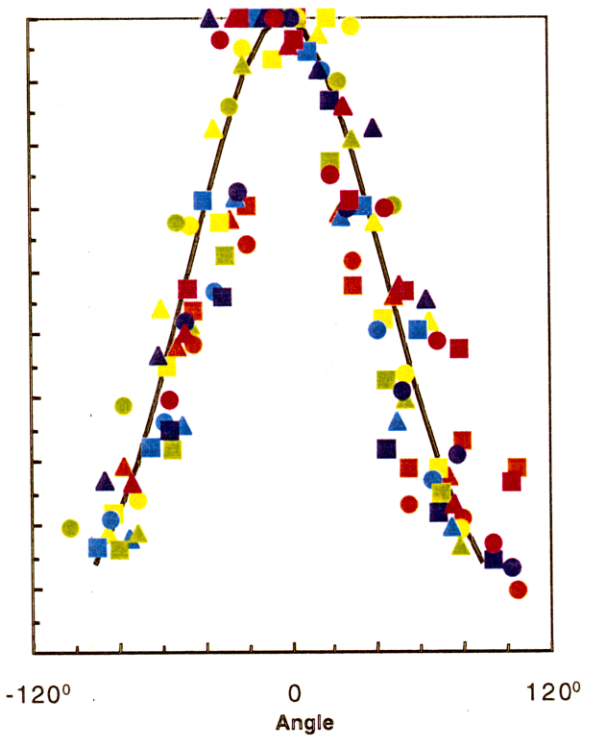

FIG.4. The angular pattern of nuclear activation recorded with a hemisphere array of gold discs. Six colors represent different shot and profiles are plotted on three axes (circles, squares, triangles) for each shot. Yield is normalized to unity at the peak and the peak direction is normalized to zero degrees to show the reproducibility of the 100° full width at half maximum. The direction of the peak varied randomly from shot to shot with a range of ± 40°.

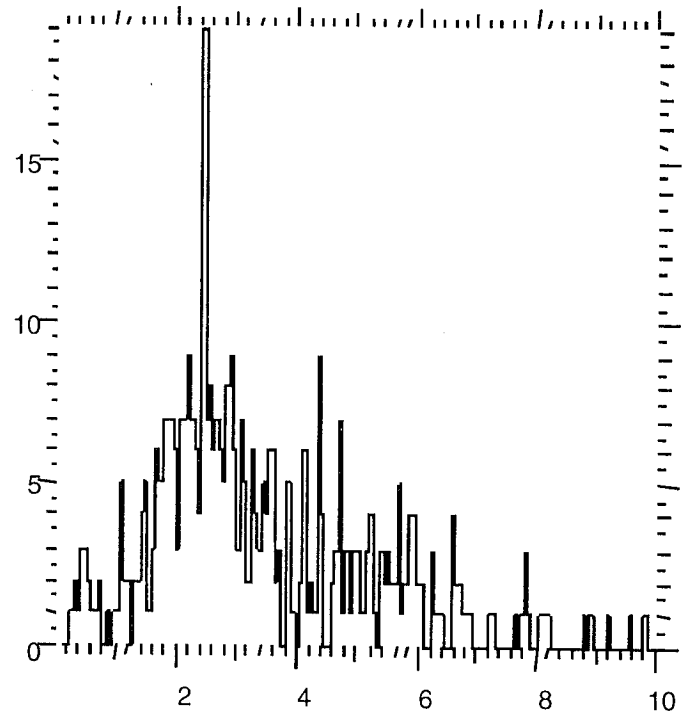

Fig. 5. Neutron energy spectrum showing counts per 0.06 MeV bin as a function of neutron energy in MeV . The narrow peak at 2.45 MeV is 4σ above the statistical noise and is attributed to thermonuclear fusion of deuterium.